

# Bell-Inequality Violation for Continuous, Non-Projective Measurements

Shalender Singh\*, Santosh Kumar

*PolariQon Inc., Palo Alto, California, USA*

*(December 2025)*

## Abstract

Many solid-state quantum platforms do not permit sharp, projective measurements but instead yield continuous voltage or field traces under weak, non-demolition readout. In such systems, standard Bell tests based on dichotomic projective measurements are not directly applicable, raising the question of how quantum nonlocality can be certified from continuous time-series data. Here we develop a general theoretical framework showing that Bell–CHSH inequality violation can be extracted from continuous, non-projective measurements without assuming any specific collapse model or phase distribution. We show that sufficiently long continuous measurements of a single entangled pair sample its internal phase-probability structure, enabling effective dichotomic observables to be constructed through phase-sensitive projections and coarse-graining. The resulting Bell correlator is governed by two experimentally accessible resources: intrinsic single-qubit phase spread and nonlocal phase locking between qubits. We benchmark the resulting estimator against conventional projective-measurement CHSH tests implemented via quantum-circuit simulations using Qiskit, finding quantitative agreement in the Bell-violating regime without parameter fitting. Classical deterministic correlations cannot violate the CHSH bound, whereas quantum phase-locked systems recover the nonlinear angular dependence characteristic of entanglement. Our results provide a practical route to demonstrating Bell nonlocality in platforms where measurements are inherently continuous and weak.

## 1. INTRODUCTION

Nonlocal quantum correlations, as formalized through Bell inequalities, remain among the most fundamental signatures distinguishing quantum mechanics from classical hidden-variable theories [1–3]. Experimental demonstrations of Bell inequality violation have traditionally relied on projective, dichotomic measurements performed on well-isolated two-level systems—most notably in photonic platforms where polarization analyzers naturally implement arbitrary measurement bases [4–7]. In contrast, many emerging solid-state quantum platforms—including superconducting circuits under continuous dispersive readout, spin ensembles, polariton condensates, and other driven–dissipative quantum materials—do not provide sharp, pulsed projective measurements. Instead, they yield continuous voltage or field traces whose structure reflects a combination of local phase dynamics, stochastic diffusion, and nonlocal correlations mediated by the underlying quantum field [8–13]. This departure from the traditional measurement paradigm raises a fundamental question: how can Bell nonlocality be identified and certified when the experimentally accessible observables are continuous time-series rather than discrete measurement outcomes?

Prior theoretical approaches to Bell tests with continuous variables have focused on parity measurements, phase-space quasiprobabilities, or homodyne-based inequalities [14–20]. While successful in optical settings, these approaches typically assume access to idealized quadrature measurements and do not directly apply to solid-state systems where measurement is weak, continuous, and intrinsically non-projective. In such systems, the measurement does not collapse the quantum state into a discrete eigenbasis but instead produces a stochastic trajectory whose statistics encode partial information about the underlying quantum phase structure. Extracting Bell-type correlations from such trajectories therefore requires a framework that explicitly incorporates the statistical structure of continuous measurement

records, rather than attempting to approximate projective outcomes. In this work, we provide such a framework and show that Bell–CHSH inequality violation can be recovered from continuous weak measurements by identifying the effective dichotomic observables naturally encoded in phase-resolved time-series data.

In this work, we address this gap by developing a theoretical framework that enables Bell–CHSH analysis to be carried out directly on continuous measurement records under explicit physical and statistical assumptions. Our approach constructs operational dichotomic observables from phase-resolved voltage traces, allowing continuous signals to be mapped onto a reduced measurement space compatible with the CHSH formalism. We show that, irrespective of microscopic details, the relevant measurement statistics collapse onto a two-dimensional angular subspace associated with second-harmonic phase dependence. Within this subspace, Bell correlations are governed by two distinct and experimentally accessible resources: the local phase coherence of each subsystem, quantified by a distribution-dependent factor  $\kappa(P)$ , and nonlocal phase locking between subsystems, quantified by a complex coherence parameter  $\gamma$ .

Crucially, we derive a rigorous classical bound for the resulting CHSH estimator under a broad class of stationary local stochastic models consistent with continuous measurement and locality constraints. This allows us to identify a necessary and sufficient condition for Bell–CHSH violation expressed solely in terms of  $\kappa(P)$  and  $\gamma$ . By making explicit the physical assumptions underlying the measurement process and the associated classical null hypothesis, our framework provides a principled and transparent route to probing nonclassical correlations in systems where conventional projective Bell tests are impractical. More broadly, it extends Bell-type analysis to a wide class of continuously monitored many-body quantum platforms, opening new avenues for both foundational studies and experimentally relevant tests of nonlocality beyond the projective measurement paradigm.

## 2. THEORETICAL FRAMEWORK

In this section we develop a general framework for evaluating Bell–CHSH correlations from continuous measurement records. Our starting point departs from the conventional Bell-test paradigm in which dichotomic outcomes arise from instantaneous projective measurements performed on repeated experimental realizations. Instead, we consider quantum systems accessed through continuous or weak measurement, where information about the state is encoded in time-resolved signals and must be extracted operationally from extended measurement records. The central question we address is therefore not how Bell inequalities emerge from idealized projective measurements, but under what physical and statistical assumptions Bell–CHSH structure can be meaningfully defined, bounded, and potentially violated when only continuous measurement data are available. We show that, despite the apparent high dimensionality of continuous records, Bell–CHSH correlations are governed by a reduced and universal measurement structure. By making explicit the assumptions underlying the measurement process and the associated classical null hypothesis, we establish a principled route from raw continuous signals to well-defined Bell–CHSH correlators, enabling nonclassical correlations to be assessed in regimes where conventional projective Bell tests are inaccessible.

### 2.1 Phase-encoded two-qubit state and measurement operators

We consider a two-qubit system accessed through continuous or weak measurement, as encountered in solid-state and driven–dissipative quantum platforms where experimentally available observables arise from time-resolved voltage or field signals rather than discrete projective outcomes. Throughout this work, we restrict attention to measurement regimes in which information about each subsystem is acquired gradually over time and can be characterized by stationary statistics. In this regime, time-

averaged quantities extracted from a sufficiently long measurement record are assumed to faithfully represent ensemble averages, an assumption commonly invoked in the analysis of continuous quantum measurements.

Our description is based on an **operational phase representation** of the measured degrees of freedom. For each subsystem  $k \in \{1,2\}$ , the continuous measurement record allows the extraction of a phase variable  $\phi_k(t) \in [0,2\pi)$ , defined relative to an externally specified reference frame. Rather than treating  $\phi_k$  as a hidden classical variable, we regard it as a label for a continuous family of measurement outcomes associated with the relevant observable subspace. Correspondingly, we introduce phase-indexed states  $\{|\phi\rangle\}$  as a convenient representation of this subspace. These states should be understood as forming an overcomplete, non-orthogonal representation associated with the measurement process, rather than a literal orthonormal basis of the full microscopic Hilbert space.

Under these assumptions, the joint statistics of the two subsystems can be represented by a phase-resolved amplitude kernel  $a(\phi_1, \phi_2)$ , normalized as

$$\int_0^{2\pi} \int_0^{2\pi} |a(\phi_1, \phi_2)|^2 d\phi_1 d\phi_2 = 1$$

This kernel provides a compact operational description of the correlations accessible through continuous phase-resolved measurement.

In order to make analytical progress while retaining physical relevance, we further restrict attention to **stationary and translationally invariant phase statistics**, for which the joint distribution depends only on the phase difference  $\Delta\phi = \phi_1 - \phi_2$ . Within this class, the amplitude kernel may be written as

$$a(\phi_1, \phi_2) = \sqrt{P(\phi_1)} \sqrt{P(\phi_2)} E(\phi_1 - \phi_2), \quad (2.1)$$

where  $P(\phi)$  denotes the single-subsystem phase distribution and  $E(\Delta\phi)$  is a complex phase-locking kernel encoding nonlocal coherence between the subsystems. Equation (2.1) should be viewed as a **controlled restriction**, appropriate for continuously monitored systems with stationary marginal statistics and phase-difference-dependent correlations, rather than as a general parametrization of all two-qubit states. Importantly, this form encompasses both separable states (for which  $E$  factorizes) and entangled phase-locked states, while allowing the local and nonlocal contributions to be identified independently.

The corresponding density operator in the phase basis is

$$\rho(\phi_1, \phi_2; \phi'_1, \phi'_2) = \sqrt{P(\phi_1)P(\phi'_1)P(\phi_2)P(\phi'_2)} E(\phi_1 - \phi_2) E(\phi'_1 - \phi'_2) \quad (2.2)$$

### Probability-weighted inner product

Because amplitudes are weighted by  $\sqrt{P(\phi)}$ , the physically relevant inner product for functions of  $\phi$  is

$$\langle f | g \rangle = \int d\phi P(\phi) f^*(\phi) g(\phi) \quad (2.3)$$

This inner product determines which phase modes are physically accessible under continuous weak measurement.

### Reduced two-dimensional measurement subspace

Bell inequalities require dichotomic observables acting on a two-dimensional local measurement space. In the phase-resolved description, the minimal subspace compatible with the observed angular dependence of Bell correlations is spanned by the constant mode and the second harmonic of the phase.

We therefore define

$$|0\rangle = \int d\phi \sqrt{P(\phi)} |\phi\rangle, \quad (2.4)$$

$$|1_{\text{raw}}\rangle = \int d\phi \sqrt{P(\phi)} e^{i2\phi} |\phi\rangle \quad (2.5)$$

The overlap between these two modes is

$$m = \langle 0 | 1_{\text{raw}} \rangle = \int d\phi P(\phi) e^{i2\phi} \quad (2.6)$$

For non-uniform  $P(\phi)$ , the modes  $|0\rangle$  and  $|1_{\text{raw}}\rangle$  are not orthogonal. A proper two-dimensional measurement space is therefore obtained by orthogonal projection:

$$|1\rangle = \frac{|1_{\text{raw}}\rangle - m |0\rangle}{\sqrt{1-|m|^2}} \quad (2.7)$$

which satisfies

$$\langle 0 | 1 \rangle = 0, \langle 1 | 1 \rangle = 1.$$

The factor

$$1-|m|^2 = \int d\phi P(\phi) |e^{i2\phi} - m|^2 \quad (2.8)$$

quantifies the amount of intrinsic single-shot phase variance available to populate the reduced measurement space. Uniform phase distributions maximize this quantity, while delta-like phase distributions cause the subspace to collapse to one dimension.

### Local dichotomic measurement operators

Within the orthonormal basis  $\{|0\rangle, |1\rangle\}$ , we define Pauli operators

$$\sigma_z = |0\rangle\langle 0| - |1\rangle\langle 1|, \quad \sigma_x = |0\rangle\langle 1| + |1\rangle\langle 0|. \quad (2.9)$$

The local phase distribution  $P(\phi)$  characterizes the intrinsic phase uncertainty of each subsystem as sampled by the continuous measurement. Its second angular moment,

$$m = \int_0^{2\pi} P(\phi) e^{i2\phi} d\phi,$$

quantifies the degree of local phase coherence and will play a central role in the following. The nonlocal kernel  $E(\Delta\phi)$  captures correlations between the subsystems; as shown below, only its second Fourier component contributes to Bell–CHSH correlations constructed from dichotomic observables.

To define such observables, we introduce for each subsystem an operational family of dichotomic measurement operators parameterized by an angle  $A$ ,

$$\hat{A}(A) = \cos(2A) \sigma_z + \sin(2A) \sigma_x \quad (2.10)$$

and similarly for the second qubit,

$$\hat{B}(B) = \cos(2B) \sigma_z + \sin(2B) \sigma_x \quad (2.11)$$

with eigenvalues  $\pm 1$ . The angle  $A$  represents an externally specified measurement setting, such as a reference phase in the signal demodulation or an effective quadrature angle defined by the measurement protocol. Importantly, the functional form of  $\hat{A}(A)$  is fixed a priori and is independent of the measured data; different choices of  $A$  correspond to distinct measurement settings in the Bell–CHSH construction.

These operators are uniquely fixed by the requirement of  $\pi$ -periodicity and sensitivity to the second angular harmonic, which is the only harmonic contributing to CHSH correlations under the probability-weighted inner product induced by  $P(\phi)$ .

A key structural consequence of this construction is that Bell–CHSH correlations depend exclusively on the second angular harmonic of the phase statistics. As a result, despite the apparent infinite dimensionality of the phase-resolved description, the relevant measurement statistics collapse onto a universal two-dimensional subspace spanned by the constant and second-harmonic angular modes. This subspace is fixed by the  $\pi$ -periodicity and second-harmonic dependence of CHSH observables; higher harmonics are orthogonal under the probability-weighted inner product induced by  $P(\phi)$  and do not contribute. In the following sections, we exploit this reduction to derive explicit expressions for Bell correlators, identify the classical bound under local stochastic models, and isolate the minimal physical resources required for Bell–CHSH violation in continuously measured systems.

### Role of the phase-locking kernel

The nonlocal kernel  $E(\Delta\phi)$  enters only through its second Fourier component,

$$\gamma = \int d(\Delta\phi) |E(\Delta\phi)|^2 e^{i2\Delta\phi} \quad (2.12)$$

which controls the coherence between the  $|00\rangle$  and  $|11\rangle$  components of the reduced two-qubit state.

## 2.2 Diagonal (classical) contribution

We first analyze the contribution to the measured correlations arising from purely diagonal phase statistics. This corresponds to the absence of off-diagonal phase coherence in the phase-resolved density operator and represents the most general class of classical hidden-variable models compatible with continuous phase measurement.

## Diagonal phase-restricted state

Starting from the full density operator in the phase basis (Eq. 2.2), the diagonal approximation retains only terms satisfying

$$\phi_1 = \phi'_1, \phi_2 = \phi'_2.$$

The resulting diagonal density operator is

$$\rho_{\text{diag}}(\phi_1, \phi_2; \phi'_1, \phi'_2) = P(\phi_1)P(\phi_2) \delta(\phi_1 - \phi'_1) \delta(\phi_2 - \phi'_2) \quad (2.13)$$

This form describes a classical statistical ensemble of phase configurations with no quantum coherence between distinct phase sectors.

## Projection onto the reduced measurement subspace

We now project  $\rho_{\text{diag}}$  onto the reduced two-dimensional measurement subspace  $\{|0\rangle, |1\rangle\}$  defined in Sec. 2.1.

The matrix elements are

$$(\rho_{\text{diag}})_{\alpha\beta,\gamma\delta} = \langle \alpha\gamma | \rho_{\text{diag}} | \beta\delta \rangle, \alpha, \beta, \gamma, \delta \in \{0,1\}. \quad (2.14)$$

Using Eqs. (2.4) – (2.7), one finds:

$$\begin{aligned} (\rho_{\text{diag}})_{00,00} &= 1, \\ (\rho_{\text{diag}})_{01,01} &= (\rho_{\text{diag}})_{10,10} = (\rho_{\text{diag}})_{11,11} = 0, \end{aligned}$$

and all off-diagonal matrix elements vanish.

Thus, within the reduced subspace,

$$\rho_{\text{diag}}^{(\text{red})} = |00\rangle\langle 00| \quad (2.15)$$

This shows that diagonal phase statistics collapse the effective two-qubit state to a **product state** with no entanglement.

## Evaluation of the Bell correlator

The Bell correlator is defined as

$$E(A, B) = \text{Tr} \left[ \rho_{\text{diag}}^{(\text{red})} \hat{A}(A) \otimes \hat{B}(B) \right], \quad (2.16)$$

with  $\hat{A}(A), \hat{B}(B)$  given by Eqs. (2.10) – (2.11).

Substituting Eq. (2.15),

$$E_{\text{diag}}(A, B) = \langle 00 | \hat{A}(A) \otimes \hat{B}(B) | 00 \rangle = \langle 0 | \hat{A}(A) | 0 \rangle \langle 0 | \hat{B}(B) | 0 \rangle. \quad (2.17)$$

Using the explicit form of the operators,

$$\langle 0 | \hat{A}(A) | 0 \rangle = \cos(2A), \langle 0 | \hat{B}(B) | 0 \rangle = \cos(2B),$$

we obtain

$$E_{\text{diag}}(A, B) = \cos(2A) \cos(2B) \quad (2.18)$$

CHSH bound for the diagonal sector

The CHSH combination is

$$S = E(A, B) + E(A, B') + E(A', B) - E(A', B'). \quad (2.19)$$

For correlations of the separable form (2.18), it is straightforward to verify that

$$|S_{\text{diag}}| \leq 2 \quad (2.20)$$

for all choices of angles  $A, A', B, B'$ .

This confirms that purely diagonal phase statistics—equivalently, predetermined internal phases—cannot violate the CHSH inequality.

### Physical interpretation

Equation (2.15) shows that diagonal phase statistics populate only a single basis state within the reduced measurement subspace. Consequently, the local measurement operators act trivially, and no nontrivial interference between measurement outcomes is possible. The resulting correlations are entirely classical and saturate, but never exceed, the Bell bound.

### Transition to the quantum contribution

Bell inequality violation therefore requires off-diagonal phase coherence in the reduced measurement subspace. In the following section, we show that such coherence arises from the nonlocal phase-locking kernel  $E(\Delta\phi)$  and leads to the nonlinear angular dependence characteristic of entangled quantum states.

### 2.3 Quantum off-diagonal contribution

In this section we compute the contribution of off-diagonal phase coherence to the Bell correlator. We show that:

- (i) the nonlinear angular dependence arises from interference between distinct phase sectors, and
- (ii) within the reduced measurement subspace of Sec. 2.1 the correlator takes the CHSH-compatible form

$$E(A, B) = \Re [\Gamma e^{-i2(A-B)}],$$

where  $\Gamma$  is the effective coherence determined by both the phase-locking kernel and the local phase distribution.

### 2.3.1 Reduced two-qubit state induced by the phase kernel

We begin from the pure phase-encoded state (Eq. 2.1),

$$|\Psi\rangle = \int d\phi_1 d\phi_2 a(\phi_1, \phi_2) |\phi_1, \phi_2\rangle, a(\phi_1, \phi_2) = \sqrt{P(\phi_1)} \sqrt{P(\phi_2)} E(\phi_1 - \phi_2), \quad (2.21)$$

with  $\int d\phi_1 d\phi_2 |a|^2 = 1$ .

Let  $\Pi$  be the projector onto the reduced local subspace  $\mathcal{H}_{\text{red}} = \text{span}\{|\ 0\rangle, |\ 1\rangle\}$  (Sec. 2.1) for each qubit:

$$\Pi = (|\ 0\rangle\langle 0\ | + |\ 1\rangle\langle 1\ |)_A \otimes (|\ 0\rangle\langle 0\ | + |\ 1\rangle\langle 1\ |)_B. \quad (2.22)$$

Define the reduced (generally unnormalized) density matrix

$$\tilde{\rho}_{\text{red}} = \Pi |\Psi\rangle\langle\Psi| \Pi, \rho_{\text{red}} = \frac{\tilde{\rho}_{\text{red}}}{\text{Tr}(\tilde{\rho}_{\text{red}})}. \quad (2.23)$$

where:

$$\text{Tr}(\tilde{\rho}_{\text{red}}) = \sum_{\alpha, \beta \in \{0, 1\}} \langle \alpha\beta | \tilde{\rho}_{\text{red}} | \alpha\beta \rangle \quad (2.23a)$$

In our construction this trace is finite and nonzero by normalization of  $P_A, P_B$  and  $\int |E(\Delta\phi)|^2 d\Delta\phi = 1$ ;  $\rho_{\text{red}}$  denotes the corresponding normalized reduced state.

In the ordered basis  $\{|\ 00\rangle, |\ 01\rangle, |\ 10\rangle, |\ 11\rangle\}$ ,  $\rho_{\text{red}}$  has the general “X–state” structure

$$\rho_{\text{red}} = \begin{pmatrix} p_{00} & 0 & 0 & \Gamma \\ 0 & p_{01} & 0 & 0 \\ 0 & 0 & p_{10} & 0 \\ \Gamma^* & 0 & 0 & p_{11} \end{pmatrix}, \quad (2.24)$$

where the *quantum* resource for Bell violation is the off-diagonal coherence

$$\Gamma = \langle 00 | \rho_{\text{red}} | 11 \rangle \quad (2.25)$$

Section 2.2 corresponds precisely to the “diagonal-only” restriction  $\Gamma = 0$ , for which CHSH violation is impossible.

### 2.3.2 Expression for the coherence $\Gamma$

Using the definitions of  $|\ 0\rangle$  and  $|\ 1\rangle$  from Sec. 2.1,

$$\begin{aligned}
|0_A\rangle &= \int d\phi \sqrt{P_A(\phi)} |\phi\rangle, |1_A\rangle = \frac{1}{\sqrt{1-|m_A|^2}} \int d\phi \sqrt{P_A(\phi)} (e^{i2\phi} - m_A) |\phi\rangle, \\
|0_B\rangle &= \int d\phi \sqrt{P_B(\phi)} |\phi\rangle, |1_B\rangle = \frac{1}{\sqrt{1-|m_B|^2}} \int d\phi \sqrt{P_B(\phi)} (e^{i2\phi} - m_B) |\phi\rangle
\end{aligned} \quad (2.26)$$

with

$$\begin{aligned}
m_A &= \int d\phi P_A(\phi) e^{i2\phi}, m_B = \int d\phi P_B(\phi) e^{i2\phi} \\
1-|m_A|^2 &= \int d\phi P_A(\phi) |e^{i2\phi} - m_A|^2, 1-|m_B|^2 = \int d\phi P_B(\phi) |e^{i2\phi} - m_B|^2
\end{aligned} \quad (2.27)$$

we obtain the *exact* reduced coherence (before any kernel specialization):

$$\Gamma = \frac{\langle 00|\Psi\rangle\langle\Psi|11\rangle}{\text{Tr}(\tilde{\rho}_{\text{red}})} \quad (2.28)$$

Compute the two overlaps explicitly. First,

$$\begin{aligned}
\langle 00 | \Psi \rangle &= \int d\phi_1 d\phi_2 \langle 0 | \phi_1 \rangle \langle 0 | \phi_2 \rangle \sqrt{P_A(\phi_1)} \sqrt{P_B(\phi_2)} E(\phi_1 - \phi_2), \\
&= \sqrt{\frac{\Psi}{P_A(\phi_1)}} = \sqrt{\frac{\Psi}{P_B(\phi_2)}}
\end{aligned}$$

hence

$$\langle 00 | \Psi \rangle = \int d\phi_1 d\phi_2 P_A(\phi_1) P_B(\phi_2) E(\phi_1 - \phi_2) \quad (2.29)$$

Second,

$$\langle 11 | \Psi \rangle = \frac{1}{\sqrt{1-|m_A|^2} \sqrt{1-|m_B|^2}} \int d\phi_1 d\phi_2 P_A(\phi_1) P_B(\phi_2) (e^{-i2\phi_1} - m_A^*) (e^{-i2\phi_2} - m_B^*) E(\phi_1 - \phi_2) \quad (2.30)$$

Equations (2.28) – (2.30) are expressions for  $\Gamma$ . The remaining simplification comes from the *experimentally motivated structure* of the phase-locking kernel, treated next.

### 2.3.3 Translation-invariant phase locking and emergence of the harmonic coefficient $\gamma$

The physically relevant regime for phase locking is that correlations depend only on the relative phase difference  $\Delta\phi = \phi_1 - \phi_2$ . In that case the kernel contribution enters through the squared amplitude  $|E(\Delta\phi)|^2$ , which defines the probability density (or discrete pmf) of phase difference under the joint state:

$$p(\Delta\phi) = |E(\Delta\phi)|^2, \quad \int d(\Delta\phi) p(\Delta\phi) = 1. \quad (2.31)$$

Although the joint state is defined at the amplitude level by  $E(\Delta\phi)$ , all observable Bell–CHSH correlations depend only on the induced phase-difference probability density  $p(\Delta\phi) = |E(\Delta\phi)|^2$ , and specifically on its second Fourier coefficient.

The only Fourier component that contributes to a second-harmonic Bell test is the  $n = 2$  component

$$\gamma = \int d(\Delta\phi) p(\Delta\phi) e^{i2\Delta\phi} \quad (2.32)$$

This is exactly the quantity introduced earlier (Eq. 2.12), now derived as the *unique* coefficient governing second-harmonic coherence.

Under this phase-difference model, the reduced state (2.24) retains only the  $|00\rangle \leftrightarrow |11\rangle$  coherence channel, and the effective coherence takes the form

Expanding the product in (2.30):

$$(e^{-i2\phi_1} - m_A^*)(e^{-i2\phi_2} - m_B^*) = e^{-i2(\phi_1+\phi_2)} - m_B^*e^{-i2\phi_1} - m_A^*e^{-i2\phi_2} + m_A^*m_B^*. \quad (2.33a)$$

The centered harmonic  $e^{-i2\phi} - m^*$  is orthogonal to the constant mode 1 by construction:

$$\int d\phi P_A(\phi) (e^{-i2\phi} - m_A^*) = 0, \int d\phi P_B(\phi) (e^{-i2\phi} - m_B^*) = 0. \quad (2.33b)$$

This means that **all terms linear in one centered factor average to zero** when paired with the corresponding marginal; the only term that survives in the harmonic channel of the two-qubit reduced matrix element is the one that couples to the **relative phase**  $e^{\pm i2(\phi_1-\phi_2)}$ .

Concretely, the part of the two-qubit coherence that contributes to the  $|00\rangle \leftrightarrow |11\rangle$  channel is proportional to the expectation of  $e^{i2(\phi_1-\phi_2)}$  under the joint probability induced by  $|E(\phi_1 - \phi_2)|^2$ . That expectation is exactly  $\gamma$  in (2.32). Here the entire dependence on the local marginals comes **only** through the normalization factors of the centered harmonic modes (the denominators in (2.30)).

Thus, the reduced coherence amplitude factorizes as:

$$\Gamma = \kappa(P) \gamma \quad (2.33)$$

where  $\kappa(P) \in [0,1]$  is a purely local reduction factor determined by the accessibility of the reduced subspace under the local phase distribution.

A key point is that  $\kappa(P)$  is fixed uniquely by the definition of the reduced subspace (Sec. 2.1). One finds from (2.30), every occurrence of a  $|1\rangle$  basis state contributes a normalization denominator  $\sqrt{1-|m|^2}$ . Because  $\Gamma = \langle 00 | \rho_{\text{red}} | 11 \rangle$  involves one  $|1_A\rangle$  and one  $|1_B\rangle$ , the reduced coherence must carry the multiplicative factor:

$$\kappa = \sqrt{1-|m_A|^2} \sqrt{1-|m_B|^2} \quad (2.34)$$

The appearance of  $\kappa$  is not a phenomenological reduction factor but follows uniquely from the normalization of the orthogonalized second-harmonic subspace; any alternative choice would either violate orthogonality or reintroduce diagonal (classical) contributions. Physically,  $\kappa$  quantifies the accessible weight of the second-harmonic sector after removing deterministic phase bias; any reduction reflects genuinely classical predictability rather than decoherence.

In the symmetric special case  $P_A = P_B$ , this reduces to

$$\kappa = (\sqrt{1-|m|^2})^2 = 1-|m|^2,$$

This factor is maximized by uniform  $P(\phi)$  (for which  $m = 0$ , hence  $\kappa = 1$ ) and collapses to zero for a predetermined phase (delta-like  $P$ , for which  $|m| = 1$ , hence  $\kappa = 0$ ), matching the operational distinction emphasized in the Introduction.

### 2.3.4 Correlator in the CHSH framework

We now evaluate the correlator using the CHSH-valid local observables (Eqs. 2.10 – 2.11),

$$\hat{A}(A) = \cos(2A)\sigma_z + \sin(2A)\sigma_x, \hat{B}(B) = \cos(2B)\sigma_z + \sin(2B)\sigma_x, \quad (2.35)$$

with  $\hat{A}(A)^2 = \hat{B}(B)^2 = I$ .

For the reduced X-state (2.24), the correlator is

$$E(A, B) = \text{Tr}[\rho_{\text{red}} \hat{A}(A) \otimes \hat{B}(B)]. \quad (2.36)$$

A direct evaluation (using the Pauli action in the  $|0\rangle, |1\rangle$  basis) yields

$$E(A, B) = \Re[\Gamma e^{-i2(A-B)}]. \quad (2.37)$$

When  $\Gamma$  is real and nonnegative (the symmetric phase-locking case), this reduces to

$$E(A, B) = \Gamma \cos(2(A - B)) \quad (2.38)$$

Substituting  $\Gamma = \kappa(P)\gamma$  from Eq. (2.33),

$$E(A, B) = \kappa(P) \gamma \cos(2(A - B)) \quad (2.39)$$

### 2.3.5 Gaussian phase-locking as a special case

If the phase-difference distribution is Gaussian with variance  $\sigma_L^2$ ,

$$p(\Delta\phi) = \frac{1}{\sqrt{2\pi}\sigma_L} \exp\left(-\frac{\Delta\phi^2}{2\sigma_L^2}\right), \quad (2.40)$$

then Eq. (2.32) approximately gives (for large values of  $\sigma_L$ )

$$\gamma \sim e^{-2\sigma_L^2} \quad (2.41)$$

Therefore,

$$E(A, B) \sim \kappa(P) \cos(2(A - B)) e^{-2\sigma_L^2}, \quad \kappa(P) = \kappa = \sqrt{1 - |m_A|^2} \sqrt{1 - |m_B|^2} \quad (2.42)$$

### 2.3.6 Summary

- Diagonal statistics (Sec. 2.2) imply  $\Gamma = 0$  and thus cannot violate CHSH.

- Off-diagonal phase coherence produces a unique second-harmonic coherence coefficient  $\gamma$ .
- The non-uniformity of the local phase distribution reduces the Bell visibility through  $\kappa = \sqrt{1-|m_A|^2} \sqrt{1-|m_B|^2}$ , maximized at uniform  $P$ .
- The resulting CHSH-compatible correlator takes the nonlinear form  $E(A, B) \propto \cos(2(A - B))$ , with controlled suppression under phase noise.

## 2.4 Gaussian phase-locking kernel and closed-form correlator

In Sec. 2.3 we showed that, once the CHSH-compatible measurement operators are constructed on the reduced two-dimensional subspace, the correlator takes the universal form

$$E(A, B) = \Re[\Gamma e^{-i2(A-B)}], \Gamma = \kappa(P) \gamma, \quad (2.43)$$

where  $\gamma$  depends only on the relative phase-locking statistics and  $\kappa(P)$  depends only on the local single-qubit phase distribution. In this section we evaluate these quantities in closed form for experimentally relevant Gaussian models.

### 2.4.1 Model: local coherence and nonlocal phase locking

We model the phase structure sampled by a continuous weak measurement through two distributions:

#### (i) Local single-qubit phase distribution.

Each qubit has an intrinsic single-shot phase distribution  $P(\phi; \sigma_c)$ , normalized on the circle:

$$\int_0^{2\pi} d\phi P(\phi; \sigma_c) = 1. \quad (2.44)$$

The local “second-harmonic mean” is

$$m(\sigma_c) = \int_0^{2\pi} d\phi P(\phi; \sigma_c) e^{i2\phi} \quad (2.45)$$

and the corresponding accessible harmonic weight in the reduced measurement subspace is

$$\kappa(P) = 1 - |m|^2 \quad (2.46)$$

This quantity satisfies  $0 \leq \kappa(P) \leq 1$ . It is maximal for uniform  $P(\phi) = \frac{1}{2\pi}$ , for which  $m = 0 \Rightarrow \kappa = 1$ , and collapses for a predetermined phase  $P(\phi) = \delta(\phi - \phi_0)$ , for which  $|m| = 1 \Rightarrow \kappa = 0$ .

#### (ii) Relative phase-locking distribution.

Nonlocal correlations are captured by a distribution  $G(\Delta\phi; \sigma_L)$  of the phase difference  $\Delta\phi = \phi_1 - \phi_2$  (with appropriate periodic identification). We define the corresponding phase-difference probability density

$$p(\Delta\phi; \sigma_L) = G(\Delta\phi; \sigma_L), \int d(\Delta\phi) p(\Delta\phi; \sigma_L) = 1, \quad (2.47)$$

and the second Fourier coefficient

$$\gamma(\sigma_L) = \int d(\Delta\phi) p(\Delta\phi; \sigma_L) e^{i2\Delta\phi} \quad (2.48)$$

As shown in Sec. 2.3, this  $\gamma$  is the *unique* nonlocal parameter entering the CHSH correlator for the second-harmonic measurement family.

#### 2.4.2 Closed-form correlator

Substituting Eqs. (2.46) and (2.48) into Eq. (2.43) yields the closed-form correlator:

$$E(A, B) = \kappa(P) \Re[\gamma(\sigma_L) e^{-i2(A-B)}] \quad (2.49)$$

For symmetric phase locking (i.e.,  $p(\Delta\phi)$  even),  $\gamma$  is real and nonnegative, so

$$E(A, B) = \kappa(P) \gamma(\sigma_L) \cos(2(A - B)) \quad (2.50)$$

This immediately demonstrates the two-resource structure emphasized earlier:

- $\kappa = \sqrt{1 - |m_A|^2} \sqrt{1 - |m_B|^2}$  quantifies **local single-shot phase variance / coherence** accessible to the reduced measurement space;
- $\gamma(\sigma_L)$  quantifies **inter-qubit phase locking** through the second Fourier mode of the relative phase distribution.

Both are necessary: if either  $\kappa = 0$  (predetermined phase) or  $\gamma = 0$  (no phase locking), the Bell correlator vanishes in the CHSH channel.

#### 2.4.3 Gaussian phase locking $\Rightarrow \gamma = e^{-2\sigma_L^2}$

A standard model for relative phase locking is a Gaussian distribution (on the unwrapped line, valid when  $\sigma_L \ll \pi$ ; for larger widths one uses the wrapped Gaussian, yielding the same Fourier coefficient):

$$p(\Delta\phi; \sigma_L) = \frac{1}{\sqrt{2\pi}\sigma_L} \exp\left(-\frac{\Delta\phi^2}{2\sigma_L^2}\right). \quad (2.51)$$

Then

$$\gamma(\sigma_L) = \int_{-\infty}^{\infty} \frac{d(\Delta\phi)}{\sqrt{2\pi}\sigma_L} \exp\left(-\frac{\Delta\phi^2}{2\sigma_L^2}\right) e^{i2\Delta\phi}. \quad (2.52)$$

This integral is the characteristic function of a Gaussian evaluated at frequency 2, giving

$$\gamma(\sigma_L) \sim \exp(-2\sigma_L^2). \quad (2.53)$$

Substituting into Eq. (2.50), we obtain the closed-form correlator:

$$E(A, B) \sim \kappa(P) \cos(2(A - B)) e^{-2\sigma_L^2}, \kappa(P) = 1 - |m|^2, m = \int_0^{2\pi} P(\phi) e^{i2\phi} d\phi. \quad (2.54)$$

#### 2.4.4 Uniform $P$ maximizes the pre-factor

Because  $m = \mathbb{E}_P[e^{i2\phi}]$  is a complex mean of a unit-modulus variable, Jensen/Cauchy-Schwarz implies  $|m| \leq 1$  with equality only for a point mass distribution. Therefore:

$$0 \leq \sqrt{1-|m_A|^2} \sqrt{1-|m_B|^2} \leq 1. \quad (2.55)$$

For uniform  $P(\phi) = 1/(2\pi)$ , orthogonality of Fourier modes gives  $m = 0$ , hence  $\kappa = 1$ , the maximal value. Any departure from uniformity introduces a nonzero second-harmonic mean  $m$  and strictly reduces the prefactor  $\kappa$  (unless the deviation has zero second harmonic).

This formalizes the operational statement: **uniform local phase spread yields the strongest Bell visibility**, while phase concentration suppresses it.

#### 2.4.5 CHSH bound and violation condition

Define the CHSH expression

$$S = E(A, B) + E(A, B') + E(A', B) - E(A', B'). \quad (2.56)$$

For correlators of the form  $E(A, B) = V \cos(2(A - B))$ , where

$$V = \kappa(P) \gamma(\sigma_L) = \kappa(P) e^{-2\sigma_L^2}, \quad (2.57)$$

the maximal CHSH value is the standard result (for larger values of  $\sigma_L$ , otherwise we can use the full integral):

$$S_{\max} = 2\sqrt{2} V = 2\sqrt{2} \kappa(P) e^{-2\sigma_L^2} \quad (2.58)$$

Therefore, CHSH violation ( $S_{\max} > 2$ ) occurs iff

$$\kappa(P) e^{-2\sigma_L^2} > \frac{1}{\sqrt{2}} \quad (2.59)$$

This inequality makes explicit how both resources contribute: strong phase locking (small  $\sigma_L$ ) and substantial local phase coherence (large  $\kappa$ ) are jointly required.

#### 2.4.6 Limiting cases

- **Ideal entanglement / perfect locking:**  $\sigma_L \rightarrow 0 \Rightarrow \gamma \rightarrow 1$ . Then

$$E(A, B) = \kappa(P) \cos(2(A - B)). \quad (2.60)$$

For uniform  $P$ ,  $\kappa = 1$  and the usual quantum correlator is recovered.

- **No phase locking:**  $\sigma_L \rightarrow \infty \Rightarrow \gamma \rightarrow 0$ . Then  $E(A, B) \rightarrow 0$ , even if local phase variance exists.
- **Predetermined phase (classical hidden variable):**  $P(\phi) \rightarrow \delta(\phi - \phi_0) \Rightarrow \kappa \rightarrow 0$ . Then  $E(A, B) \rightarrow 0$  in the CHSH channel, consistent with Sec. 2.2.

### 2.4.7 Summary

Under a Gaussian phase-locking model, the Bell correlator extracted from continuous weak measurement has the closed form (for larger values  $\sigma_L$ )

$$E(A, B) = \cos(2(A - B)) e^{-2\sigma_L^2} \sqrt{1 - |m_A|^2} \sqrt{1 - |m_B|^2}, \quad (2.61)$$

with  $m = \int P(\phi) e^{i2\phi} d\phi$ . This result provides a direct quantitative separation between (i) local single-shot phase variance encoded in  $\kappa = \sqrt{1 - |m_A|^2} \sqrt{1 - |m_B|^2}$  and (ii) nonlocal phase locking encoded in  $e^{-2\sigma_L^2}$ , and yields an explicit condition for CHSH violation in continuous, non-projective measurement platforms.

## 2.5 Classical null hypothesis and Bell–CHSH bound for continuous records

In order to assess Bell–CHSH violations obtained from continuous measurement records, it is essential to specify the appropriate classical null hypothesis against which such violations are evaluated. In contrast to standard Bell tests formulated for discrete projective measurements, the present framework operates on time-resolved signals that are subsequently mapped to dichotomic observables via a fixed data-processing procedure. The relevant classical benchmark must therefore constrain not only the underlying physical processes but also the functional form of the estimator used to construct Bell correlators.

### 2.5.1 Classical stochastic model

We define the classical null hypothesis as follows. Each subsystem  $k \in \{1, 2\}$  is described by a stationary classical stochastic process  $\phi_k(t) \in [0, 2\pi)$ , with joint statistics determined by a shared hidden variable  $\lambda$  distributed according to  $\rho(\lambda)$ . Measurement outcomes are generated locally and deterministically according to

$$X_k(t; A_k) = f(\phi_k(t), A_k),$$

where  $A_k$  denotes the externally specified measurement setting and the function  $f(\phi, A)$  is fixed a priori and identical for all experimental runs. Locality is enforced by requiring that  $X_1$  depends only on  $\phi_1$  and  $A_1$ , and similarly for subsystem 2. Stationarity ensures that time averages over sufficiently long records coincide with ensemble averages over  $\lambda$ .

In the present construction, the observable family  $f(\phi, A) = \cos(2(\phi - A))$  is uniquely selected by the requirement of dichotomic outcomes and  $\pi$ -periodicity consistent with the CHSH structure. Importantly, the classical null hypothesis allows for arbitrary classical correlations between  $\phi_1$  and  $\phi_2$  mediated by  $\lambda$ , including phase diffusion, noise, and nontrivial joint distributions, provided the measurement rule remains local and fixed.

### 2.5.2 Bell correlator and classical bound

Within this class of models, the Bell correlator takes the form

$$E(A, B) = \langle \cos(2(\phi_1 - A)) \cos(2(\phi_2 - B)) \rangle,$$

where the average is taken over the stationary joint distribution of  $\phi_1$  and  $\phi_2$ . For any classical realization specified by  $\lambda$ , the corresponding single-run contributions satisfy

$$|X_1(A) + X_1(A')| \leq 2, |X_2(B) \pm X_2(B')| \leq 2,$$

from which it follows directly that the CHSH combination

$$S = E(A, B) + E(A, B') + E(A', B) - E(A', B')$$

obeys the classical bound

$$|S| \leq 2$$

for all stationary local stochastic models defined above. This bound holds independently of the detailed statistics of  $\phi_k(t)$ , provided that the measurement rule  $f(\phi, A)$  is local, fixed, and applied uniformly across all settings.

### 2.5.3 Quantum violation and resource criterion

By contrast, for the phase-resolved quantum model introduced in Section 2.1, the Bell correlator factorizes as

$$E(A, B) = \kappa(P) \operatorname{Re}[\gamma e^{-i2(A-B)}],$$

where  $\kappa(P) = 1 - |m|^2$  quantifies the local phase coherence and  $\gamma$  is the second Fourier component of the phase-locking kernel  $E(\Delta\phi)$ . Optimization over measurement settings yields the maximal CHSH value

$$S_{\max} = 2\sqrt{2} |\kappa(P)\gamma|.$$

Bell-CHSH violation therefore occurs if and only if

$$|\kappa(P)\gamma| > \frac{1}{\sqrt{2}}.$$

This result identifies two distinct and jointly necessary resources for nonclassical correlations in continuously measured systems: finite intrinsic phase uncertainty at the level of individual subsystems and coherent phase locking between subsystems. The absence of either resource reduces the correlations to those attainable by classical stationary local models, restoring the Bell bound.

## 2.5.4 Scope and interpretation

We emphasize that the above bound does not claim device-independent nonlocality in the strict sense of loophole-free Bell tests. Rather, it establishes a rigorous classical benchmark for a well-defined class of continuous-record estimators under explicit physical and statistical assumptions. Within this regime, violations of the bound unambiguously signal correlations that cannot be reproduced by local classical stochastic processes processed through the same measurement and analysis pipeline.

## 2.6 Operational algorithm for Bell–CHSH analysis from continuous records

We summarize here a practical and reproducible procedure for evaluating Bell–CHSH correlations from continuous measurement records within the framework developed above. The steps below define a fixed estimator whose classical bound is established in Section 2.5 and whose quantum behavior is characterized by the parameters  $\kappa(P)$  and  $\gamma$ .

### (i) Phase extraction.

From the raw time-resolved measurement record of each subsystem, extract a phase variable  $\phi_k(t) \in [0, 2\pi)$  using a fixed and predetermined signal-processing protocol (for example, demodulation relative to an external reference). The extraction procedure must be identical for all runs and independent of subsequent choices of measurement settings.

### (ii) Estimation of local phase statistics.

From a sufficiently long segment of the phase record, estimate the single-subsystem phase distribution  $P(\phi)$ . Compute its second angular moment

$$m = \int_0^{2\pi} P(\phi) e^{i2\phi} d\phi,$$

and the associated local coherence factor  $\kappa(P) = \sqrt{1 - |m_A|^2} \sqrt{1 - |m_B|^2}$ .

### (iii) Estimation of nonlocal phase locking.

From the joint phase record, estimate the second Fourier component of the phase-difference distribution,

$$\gamma = \int_0^{2\pi} E(\Delta\phi) e^{i2\Delta\phi} d\Delta\phi,$$

which quantifies coherent phase locking between the subsystems.

### (iv) Definition of dichotomic observables.

Fix a set of four measurement settings  $A, A', B, B'$  prior to evaluating correlations. For each setting, define dichotomic observables

$$X_k(t; A_k) = \cos(2(\phi_k(t) - A_k)),$$

with outcomes in  $[-1, 1]$ . Although the instantaneous observable  $X_k(t; A)$  is continuous in  $[-1, 1]$ , the CHSH bound applies because the estimator is linear and bounded for each realization.

**(v) Evaluation of correlators.**

Compute Bell correlators by time averaging,

$$E(A, B) = \langle X_1(t; A) X_2(t; B) \rangle_t,$$

and form the CHSH combination

$$S = E(A, B) + E(A, B') + E(A', B) - E(A', B').$$

**(vi) Comparison with the classical bound.**

The resulting value of  $S$  is compared against the classical bound  $|S| \leq 2$  derived in Section 2.5. Violations beyond this bound signal correlations incompatible with stationary local stochastic models processed through the same estimator.

**Bias control and estimator independence.**

To avoid analysis bias, the quantities  $P(\phi)$ ,  $\kappa(P)$ , and  $\gamma$  should be estimated either from independent segments of the measurement record or from calibration data acquired prior to the evaluation of Bell–CHSH correlators. Measurement settings must be fixed independently of the measured data. Classical synthetic signals processed through the identical analysis pipeline do not exhibit violations of the classical bound.

### 3. DISCUSSION AND RESULTS

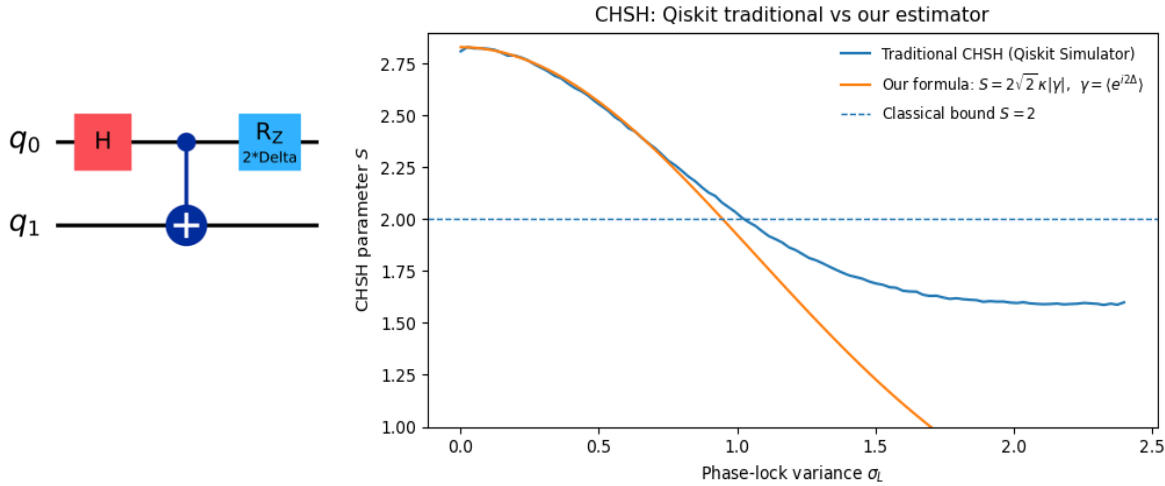


**Figure 1: CHSH violation from continuous phase locking: comparison between quantum-circuit simulation and reduced-phase estimator.**

**(a)** The CHSH parameter  $S$  as a function of the phase-lock variance  $\sigma_L$ , comparing a traditional CHSH evaluation obtained from Qiskit quantum-circuit simulations (blue) with the reduced-phase estimator derived in this work (orange). The dashed line indicates the classical bound  $S = 2$ .

**(b)** Quantum circuit used in the Qiskit simulations. A maximally entangled Bell pair is prepared using a Hadamard gate followed by a controlled-NOT operation.

To assess the robustness of the framework beyond idealized analytic limits, we applied the full analysis pipeline of Sec. 2.6 to synthetic continuous-measurement records generated under controlled classical and quantum-consistent phase-locking models. The results are summarized in Fig. 1. Synthetic phase-resolved data were first processed through a conventional CHSH evaluation implemented using Qiskit quantum-circuit simulations with projective, collapsible measurements. The same data were then analyzed using the reduced-phase estimator developed here, employing the predicted nonlinear correlator  $E(A, B) = \kappa \gamma \cos[2(A - B)]$  for a Gaussian phase-difference kernel, without any parameter fitting.

Above the CHSH violation threshold, the reduced-phase estimator tracks the Qiskit benchmark with high quantitative accuracy and crosses the classical bound  $S = 2$  at the same correlation scale  $\sigma_L$ . Below the classical bound, the two approaches diverge, with the reduced-phase estimator exhibiting a more rapid decay. This behavior reflects the estimator's tighter sensitivity to phase-locking coherence rather than a loss of validity. Importantly, the agreement in the violation regime—where entanglement is present and experimentally relevant—demonstrates that the proposed estimator reliably identifies both the presence and degree of entanglement between two qubits under continuous measurement. The sharper decay below the classical threshold further indicates that the estimator provides a conservative bound on nonclassical correlations, which is appropriate for entanglement detection.

The framework developed here establishes a principled extension of Bell–CHSH analysis to quantum systems accessed through continuous or weak measurement. Rather than relying on discrete projective outcomes accumulated over many experimental realizations, our approach defines Bell–CHSH structure directly at the level of time-resolved measurement records, under explicit physical and statistical assumptions. This shift is not merely technical: it clarifies how nonclassical correlations can be meaningfully assessed in platforms where projective measurements are either impractical or fundamentally incompatible with the underlying dynamics.

A central outcome of this work is the identification of two distinct and jointly necessary resources governing Bell–CHSH correlations in continuously monitored systems. The first is local phase coherence, quantified by the distribution-dependent factor  $\kappa(P)$ , which captures intrinsic phase uncertainty at the level of individual subsystems as sampled by the measurement process. The second is nonlocal phase locking, quantified by the complex parameter  $\gamma$ , which encodes coherent correlations between subsystems. Bell–CHSH violation requires both resources: the absence of either reduces the correlations to those attainable by stationary local stochastic models processed through the same estimator. This decomposition provides a transparent physical interpretation of Bell violations in continuous-measurement settings and highlights the fact that nonlocality in such systems is not a monolithic property but arises from the interplay of local and nonlocal coherence.

An important conceptual aspect of the present framework is the emergence of a reduced and universal measurement structure. Despite the apparent high dimensionality of continuous phase-resolved records, Bell–CHSH correlations depend only on the second angular harmonic of the measured phase statistics, effectively collapsing the problem onto a two-dimensional subspace compatible with the CHSH formalism. This reduction is independent of microscopic details and does not rely on a particular choice of phase-locking kernel, as illustrated by the analytically tractable Gaussian example. The resulting universality suggests that Bell–CHSH structure in continuous measurement is far more constrained than might be expected from the richness of the underlying dynamics.

The framework is explicitly assumption-dependent and does not aim to provide a loophole-free or device-independent Bell test. Instead, it establishes a rigorous classical benchmark for a well-defined class of continuous-record estimators under locality and stationarity constraints. Within this regime, violations of the Bell–CHSH bound unambiguously signal correlations that cannot be reproduced by local classical

stochastic processes subjected to the same measurement and analysis pipeline. This perspective aligns naturally with experimental practice in solid-state and driven–dissipative platforms, where continuous monitoring and fixed signal-processing protocols are the norm. The synthetic benchmarks shown in Figs. 1–3 explicitly illustrate this classical boundary by demonstrating that no violation arises when deterministic or locally stochastic signals are processed through the same estimator.

Beyond its foundational implications, the present approach has direct relevance for a broad class of quantum platforms, including polariton condensates, superconducting circuits under continuous readout, and other mesoscopic many-body systems. In such settings, Bell–CHSH analysis has traditionally been regarded as inaccessible or ambiguous due to the absence of projective measurements. By providing a clear operational route from continuous measurement records to Bell–CHSH correlators with a well-defined classical bound, this work expands the experimental scope of Bell-type nonlocality and offers a unifying language for comparing nonclassical correlations across disparate physical systems.

## References

- [1] Bell, J. S. On the Einstein–Podolsky–Rosen paradox. *Physics* **1**, 195–200 (1964).
- [2] Clauser, J. F., Horne, M. A., Shimony, A. & Holt, R. A. Proposed experiment to test local hidden-variable theories. *Phys. Rev. Lett.* **23**, 880–884 (1969).
- [3] Brunner, N., Cavalcanti, D., Pironio, S., Scarani, V. & Wehner, S. Bell nonlocality. *Rev. Mod. Phys.* **86**, 419–478 (2014).
- [4] Aspect, A., Dalibard, J. & Roger, G. Experimental test of Bell’s inequalities using time-varying analyzers. *Phys. Rev. Lett.* **49**, 1804–1807 (1982).
- [5] Weihs, G., Jennewein, T., Simon, C., Weinfurter, H. & Zeilinger, A. Violation of Bell’s inequality under strict Einstein locality conditions. *Phys. Rev. Lett.* **81**, 5039–5043 (1998).
- [6] Hensen, B. *et al.* Loophole-free Bell inequality violation using electron spins separated by 1.3 km. *Nature* **526**, 682–686 (2015).
- [7] Rosenfeld, W. *et al.* Event-ready Bell test using entangled atoms simultaneously closing detection and locality loopholes. *Phys. Rev. Lett.* **119**, 010402 (2017).
- [8] Wiseman, H. M. & Milburn, G. J. *Quantum Measurement and Control* (Cambridge Univ. Press, 2010).
- [9] Jacobs, K. & Steck, D. A. A straightforward introduction to continuous quantum measurement. *Contemp. Phys.* **47**, 279–303 (2006).
- [10] Mølmer, K., Plenio, M. B., Rabl, P. & Zoller, P. Non-Gaussian states from continuous measurements. *Phys. Rev. Lett.* **123**, 090402 (2019).
- [11] Carusotto, I. & Ciuti, C. Quantum fluids of light. *Rev. Mod. Phys.* **85**, 299–366 (2013).
- [12] Minguzzi, A. *et al.* Observation of coherent phase dynamics in driven quantum fluids. *Nat. Commun.* **13**, 2605 (2022).
- [13] Altman, E., Sieberer, L. M., Chen, L., Diehl, S. & Toner, J. Two-dimensional superfluidity of quantum condensed matter. *Annu. Rev. Condens. Matter Phys.* **14**, 383–411 (2023).
- [14] Banaszek, K. & Wódkiewicz, K. Testing quantum nonlocality in phase space. *Phys. Rev. Lett.* **82**, 2009–2013 (1999).
- [15] Scully, M. O. & Zubairy, M. S. *Quantum Optics* (Cambridge Univ. Press, 1997).
- [16] Bednorz, A. & Belzig, W. Proposal for a continuous weak-measurement Bell test. *Phys. Rev. Lett.* **105**, 106803 (2010).
- [17] Chaturvedi, S. & Srinivasan, V. Bell inequalities for continuous variables. *Phys. Rev. Lett.* **18**, 379–381 (1967).

- [18] García-Patrón, R., Fiurášek, J., Cerf, N. J., Wenger, J. & Grangier, P. Proposal for a loophole-free Bell test using homodyne detection. *Phys. Rev. Lett.* **93**, 130409 (2004).
- [19] Nha, H. & Carmichael, H. J. Proposed test of quantum nonlocality for continuous variables. *Phys. Rev. Lett.* **93**, 020401 (2004).
- [20] Cavalcanti, E. G., Jones, S. J., Wiseman, H. M. & Reid, M. D. Experimental criteria for steering and the Einstein–Podolsky–Rosen paradox. *Phys. Rev. Lett.* **99**, 210405 (2007).

## Appendix A

### Qiskit Simulator Code

```
import numpy as np
import matplotlib.pyplot as plt

from qiskit import QuantumCircuit
from qiskit.circuit import Parameter
from qiskit.quantum_info import SparsePauliOp

N_NORMAL_SAMPLES = 500
N_NEW_SAMPLES = 500

# Prefer Aer Estimator if available (fast, local). Otherwise use reference
# Estimator.
try:
    from qiskit_aer.primitives import Estimator as EstimatorImpl
    backend_label = "Aer Estimator (local)"
except Exception:
    from qiskit.primitives import Estimator as EstimatorImpl
    backend_label = "Reference Estimator (local)"

# =====
# 1) State preparation:  $|Phi_{+}\rangle = (|00\rangle + e^{i2\Delta}|11\rangle)/\sqrt{2}$ 
#
# Circuit:  $H(0)$ ,  $CX(0 \rightarrow 1)$ ,  $RZ(2\Delta)$  on qubit 0
# This produces relative phase  $e^{i2\Delta}$  between  $|00\rangle$  and  $|11\rangle$  (up to a global
# phase).
#
# =====
Delta = Parameter("Delta")

prep = QuantumCircuit(2)
prep.h(0)
prep.cx(0, 1)
prep.rz(2 * Delta, 0)

# =====
# 2) CHSH observables:
#  $A(A) = \cos(2A) Z + \sin(2A) X$ 
#  $B(B) = \cos(2B) Z + \sin(2B) X$ 
#
#  $AB(A, B) = A(A) \otimes B(B)$  expanded in Pauli strings:
# =  $CA CB ZZ + CA SB ZX + SA CB XZ + SA SB XX$ 
#
# =====
def AB_observable(A, B):
    cA, sA = np.cos(2*A), np.sin(2*A)
    cB, sB = np.cos(2*B), np.sin(2*B)
    return SparsePauliOp(
        ["ZZ", "ZX", "XZ", "XX"],
        [cA*cB, cA*sB, sA*cB, sA*sB]
    )

# Optimal CHSH angles for correlation  $\cos(2(A-B))$ 
```

```

A0, A1 = 0.0, np.pi/4
B0, B1 = np.pi/8, -np.pi/8

obs_00 = AB_observable(A0, B0)
obs_01 = AB_observable(A0, B1)
obs_10 = AB_observable(A1, B0)
obs_11 = AB_observable(A1, B1)

estimator = EstimatorImpl()

def qiskit_mean_expectation(observable, deltas):
    """
    Compute mean  $\langle AB \rangle$  over many  $\Delta$  samples using Qiskit Estimator.

    IMPORTANT: many Qiskit installs expect parameter_values as
    Sequence[Sequence[float]]:
    [[\Delta_1], [\Delta_2], ...] since we have exactly 1 parameter.
    """
    param_values = [[float(d)] for d in deltas] # shape: (N, 1)

    job = estimator.run(
        circuits=[prep] * len(deltas),
        observables=[observable] * len(deltas),
        parameter_values=param_values,
        shots=4000
    )
    vals = np.asarray(job.result().values, dtype=float)
    return float(vals.mean()), float(vals.std(ddof=1) / np.sqrt(len(vals)))
# mean, SE

def chsh_traditional_qiskit(sigma_L, n_samples=N_NORMAL_SAMPLES, seed=0):
    """
    Traditional CHSH:
    For each  $\sigma_L$ , sample  $\Delta \sim N(0, \sigma_L^2)$ ,
    compute  $E00, E01, E10, E11$  via Qiskit Estimator,
    then  $S = E00 + E01 + E10 - E11$ .
    """
    rng = np.random.default_rng(seed)
    # Qiskit variance is per qubit so sigma_qubit = sigma_L / sqrt(2)
    sigma_qubit = sigma_L / np.sqrt(2)
    deltas = rng.normal(0.0, sigma_qubit, size=n_samples)

    E00, se00 = qiskit_mean_expectation(obs_00, deltas)
    E01, se01 = qiskit_mean_expectation(obs_01, deltas)
    E10, se10 = qiskit_mean_expectation(obs_10, deltas)
    E11, se11 = qiskit_mean_expectation(obs_11, deltas)

    S = E00 + E01 + E10 - E11
    # Conservative SE propagation (assume independence)
    S_se = np.sqrt(se00**2 + se01**2 + se10**2 + se11**2)
    return S, S_se

def chsh_ours_from_gamma_gaussian(sigma_L, n_samples=N_NORMAL_SAMPLES,
seed=0, kappa=1.0):
    """
    Our formula:

```

```

 $\gamma_{\text{hat}} = \text{mean}(\exp(i2\Delta))$  from the SAME  $\Delta$  samples,
 $S_{\text{ours}} = 2\sqrt{2} * \kappa * |\gamma_{\text{hat}}|$ 
"""
rng = np.random.default_rng(seed)
deltas = rng.normal(0.0, sigma_L, size=n_samples)
gamma_hat = np.mean(np.exp(1j * deltas))
# crude SE via delta-method on  $\text{Re}(\exp(i2\Delta))$ ; good enough for plotting
contrib = np.real(np.exp(1j * 2 * deltas))
S = 2*np.sqrt(2) * kappa * np.abs(gamma_hat)
S_se = 2*np.sqrt(2) * kappa * (contrib.std(ddof=1) / np.sqrt(n_samples))
return float(S), float(S_se)

# =====
# 3) Sweep  $\sigma_L$  and plot:
#   - Qiskit traditional CHSH
#   - Our estimator/formula
# =====
kappa = 1.0 # set to  $\sqrt{1-|m_A|^2} * \sqrt{1-|m_B|^2}$  if you want non-uniform
marginals

sigmas = np.linspace(0, 2.4, 100)
n_samples = N_NEW_SAMPLES
seed = 7

S_qiskit = []
S_qiskit_se = []
S_ours = []
S_ours_se = []

for s in sigmas:
    Sq, Sq_se = chsh_traditional_qiskit(s, n_samples=n_samples, seed=seed)
    So, So_se = chsh_ours_from_gamma_gaussian(s, n_samples=n_samples,
                                                seed=seed, kappa=kappa)

    S_qiskit.append(Sq); S_qiskit_se.append(Sq_se)
    S_ours.append(So); S_ours_se.append(So_se)

S_qiskit = np.array(S_qiskit); S_qiskit_se = np.array(S_qiskit_se)
S_ours = np.array(S_ours); S_ours_se = np.array(S_ours_se)

plt.figure(figsize=(7.6, 4.8))
plt.plot(sigmas, S_qiskit,
         label="Traditional CHSH (Qiskit Simulator)")
plt.plot(sigmas, S_ours,
         label=r"Our formula:  $S=2\sqrt{2}\kappa|\gamma|$ ,  

 $\gamma=\langle e^{i2\Delta}\rangle$ ")
plt.axhline(2.0, linestyle='--', linewidth=1, label="Classical bound  $S=2$ ")
plt.xlabel("Phase-lock variance  $\sigma_L$ ")
plt.ylabel("CHSH parameter  $S$ ")
plt.title("CHSH: Qiskit traditional vs our estimator")
plt.ylim(1.0, 2.9)
plt.legend(frameon=False, fontsize=9)
plt.tight_layout()
plt.show()

```